

**Chronic Arsenic Exposure and Angiogenesis in  
Human Bronchial Epithelial Cells via  
the ROS/miR-199a-5p/HIF-1 $\alpha$ /COX-2 Pathway**

**Jun He, Min Wang, Yue Jiang, Qiudan Chen, Shaohua Xu,  
Qing Xu, Bing-Hua Jiang, and Ling-Zhi Liu**

**<http://dx.doi.org/10.1289/ehp.1307545>**

**Received: 25 August 2013**

**Accepted: 6 January 2014**

**Advance Publication: 10 January 2014**

# Chronic Arsenic Exposure and Angiogenesis in Human Bronchial Epithelial Cells via the ROS/miR-199a-5p/HIF-1 $\alpha$ /COX-2 Pathway

Jun He,<sup>1,2</sup> Min Wang,<sup>1</sup> Yue Jiang,<sup>3</sup> Qiudan Chen<sup>1</sup>, Shaohua Xu,<sup>4</sup> Qing Xu,<sup>2</sup> Bing-Hua Jiang,<sup>1</sup> and Ling-Zhi Liu<sup>2</sup>

<sup>1</sup>State Key Lab of Reproductive Medicine, and Department of Pathology, Nanjing Medical University, Nanjing, People's Republic of China; <sup>2</sup>Department of Pathology, Anatomy and Cell Biology, Thomas Jefferson University, Philadelphia, Pennsylvania, USA; <sup>3</sup>Faculty of Software, and College of Life Sciences, Fujian Normal University, People's Republic of China;

<sup>4</sup>Changzhou Maternal and Child Care Hospital, Changzhou, People's Republic of China

**Address correspondence to** Bing-Hua Jiang, Thomas Jefferson University, 1020 Locust Street, Philadelphia, Pennsylvania 19107 USA. Telephone: 215-503-6147. E-mail:

[binghjiang@yahoo.com](mailto:binghjiang@yahoo.com); [bhjiang@jefferson.edu](mailto:bhjiang@jefferson.edu). Ling-Zhi Liu, Thomas Jefferson University, 1020 Locust St., Philadelphia, Pennsylvania 19107 USA. Telephone: 215-503-6148. E-mail:

[Ling-Zhi.Liu@jefferson.edu](mailto:Ling-Zhi.Liu@jefferson.edu)

**Running title:** miR-199a-5p in arsenic-induced tumor angiogenesis

**Acknowledgment:** This work was supported in part by National Natural Science Foundation of China (81071642 and 30871296), Jiangsu Province's Key Discipline of Medicine (XK201117), and by NIEHS, National Institutes of Health grant (R01ES020868).

**Competing Financial Interests:** All authors declare they have no actual or potential competing financial interests.

## Abstract

**Background:** Environmental and occupational exposure to arsenic is a major public health concern. Although it has been identified as a human carcinogen, the molecular mechanism underlying the arsenic-induced carcinogenesis is not well understood.

**Objectives:** We aim to determine the role and mechanisms of miRNAs in arsenic-induced tumor angiogenesis and tumor growth.

**Methods:** We utilized an *in vitro* model by transforming human lung epithelial BEAS-2B cells through long-term exposure to arsenic. Human xenograft tumor model was established to assess tumor angiogenesis and tumor growth *in vivo*. Tube formation assay and CAM assay were used to assess tumor angiogenesis.

**Results:** We found that miR-199a-5p expression levels were more than 100-fold lower in arsenic-transformed cells than parental cells. Re-expression of miR-199a-5p impaired arsenic-induced angiogenesis and tumor growth through direct targets HIF-1 $\alpha$  and COX-2. We further showed that arsenic induced COX-2 expression through HIF-1 regulation at the transcriptional level. In addition, we demonstrated that reactive oxygen species (ROS) are an upstream event of miR-199a-5p/ HIF-1 $\alpha$ /COX-2 pathway in arsenic-induced carcinogenesis.

**Conclusion:** The findings establish critical roles of miR-199a-5p and its downstream targets HIF-1/COX-2 in arsenic-induced tumor growth and angiogenesis.

## Introduction

Arsenic is a widely distributed semimetallic element that occurs naturally in various compounds in the crust of earth. It is estimated about 160 million people worldwide are exposed to unsafe high levels of arsenic in drinking water (Hubaux et al. 2013). Of particular, about 25 million people in Bangladesh and 6 million people in India are chronically exposed to very high level of arsenic exceeding 50  $\mu\text{g/L}$  through ground water (Rahman et al. 2001), significantly greater than current maximum contaminant level (MCL) of 10  $\mu\text{g/L}$  set forth by the U.S. Environmental Protection Agency (EPA) (<http://water.epa.gov/drink/contaminants/index.cfm#two>). Long-term arsenic exposure leads to an increased risk of skin, bladder, liver cancers, especially lung cancer. Epidemiological investigations and laboratory studies have provided evidence that ingestion of arsenic via drinking water or inhalation of air increases the risk of lung cancer in a dose-response way (Boffetta 2004; Chen et al. 2004). However, the exact mechanism of arsenic-induced cell malignant transformation and cancer development remains to be investigated.

Current proposed mechanisms underlying arsenic carcinogenesis include arsenic-induced genetic changes and epigenetic alterations (Hubaux et al. 2013). The epigenetic alterations consist of histone modification, DNA methylation and miRNA regulations. We and others have observed aberrant miRNA expression profiles upon heavy-metal exposure in various cell types, an indication of the involvement of miRNAs in environmental carcinogenesis (Beezhold et al. 2011; He et al. 2013b; Wang et al. 2011). However, it remains to be determined whether these miRNAs play causal roles in arsenic-induced tumor initiation and development.

Angiogenesis is the formation of new blood vessels from existing vasculatures to induce tumor growth. Except for its role in physiological process such as embryo development and wound

healing, angiogenesis is required for cancer development. It is a critical process for a tumor colony to grow and become invasive (D'Amico 2004). In this study, we aim to determine: 1) roles of miRNAs in arsenic-induced tumor angiogenesis and tumor growth; 2) direct targets of miRNAs in regulating tumorigenesis; and 3) functional relevant angiogenesis factors in arsenic- and miRNA-mediated carcinogenesis.

## **Material and Methods**

### **Cell culture and generation of stable cell lines**

Human bronchial epithelial BEAS-2B cells (American Type Culture Collection (ATCC), Manassas, VA, USA) were cultured in DMEM medium (Invitrogen, Carlsbad, CA) supplemented with 10% fetal bovine serum (FBS). Human umbilical vein endothelial cells (HUVEC) (purchased from ATCC) were cultured in EBM-2 complete medium. AsT (arsenic-transformed BEAS-2B) cells (Carpenter et al. 2011) stably overexpressing miR-199a or miR-control were generated by infecting with lentivirus carrying miR-199a-RFP or a negative control precursor (Applied Biosystem, Austin, TX, USA), followed by the selection with puromycin. To establish stable cell lines overexpressing COX-2, 293T cells were transfected with lentivirus carrying COX-2 plasmid (GeneCopoeia, Rockville, MD, USA) or empty vector to generate infectious virus. Then AsT cells were transduced with virus, followed by the puromycin selection.

### **Animal experiment**

Female CrTac:NCr-*Foxn1*<sup>tmu</sup> mice (8-weeks-old) were purchased from Taconic (Hudson, NY, USA), and maintained in pathogen-free conditions. Animals were housed in sterilized cages (5 mice/cage) that were bedded with hardwood chips. Standardized commercial diets were

provided, and sterilized water was available at all times. The average weight of animals on the arrival was  $20 \pm 2$  g (mean  $\pm$  SD). Total  $2 \times 10^6$  AsT/miR-cont cells or AsT/miR-199a cells (AsT cells stably overexpressing miR-control or miR-199a) in 80  $\mu$ l were injected subcutaneously into the flanks of nude mice (n = 10/group). Animals used in research have been treated humanely according to Institutional Animal Care and Use Committee, Thomas Jefferson University. The mice were euthanized by decapitation 6 weeks after injection. Tumor tissues were removed, and weighed. The parts of tissues were for paraffin-embedded, other parts were snap-frozen in liquid nitrogen and stored at  $-80^\circ\text{C}$  for immunohistochemical analysis.

### **Reagents and antibodies**

Sodium arsenic ( $\text{NaAsO}_2$ ), catalase and  $\text{H}_2\text{O}_2$  were purchased from Sigma-Aldrich (St. Louis, MO, USA). SiRNA Smartpools (pool of four individual siRNAs) against COX-2, HIF-1 $\alpha$ , and scrambled control were from Dharmacon (Lafayette, CO, USA). COX-2 antibody was from Cell Signaling Technology (Beverly, MA, USA). CD31 antibody for analyzing paraffin-embedded tissues was from Santa Cruz Biotechnology (Santa Cruz, CA, USA) and for analyzing frozen tissues was from BD Pharmingen (San Jose, CA, USA). HIF-1 $\alpha$  antibody was from BD Bioscience (Franklin Lakes, NJ), and  $\alpha$ -SMA antibody was obtained from Abcam (Cambridge, MA, USA). Primary antibodies used for Western-blotting were diluted in 1:1000 in 5% BSA as working concentration, and were incubated on a shaker overnight at  $4^\circ\text{C}$ .

### **RT-qPCR analysis**

Total RNAs were extracted using Trizol (Life technologies, Carlsbad, CA). The synthesis of cDNA was performed using oligo (dT)18 primers and M-MLV reverse transcriptase (Promega, Madison, WI, USA). The amplification was performed by PCR. SYBR-Green RT-qPCR was

performed to detect COX-2 and GAPDH mRNA levels using Power SYBR Green PCR Master Mix Kit (Applied Biosystems, Carlsbad, CA, USA). Taqman RT-qPCR was performed to detect miRNA expression levels using Taqman miRNA reverse transcription kit and Taqman universal PCR master mix (Applied Biosystems, Austin, TX, USA). The primer sequences are listed below:

Primers for SYBR-Green RT-qPCR

COX-2 forward: 5'-TCAGCCATACAGCAAATCCTT-3'

COX-2 reverse: 5'-CTGCACTGTGTTAGTGG-3'

GAPDH forward: 5'-ATGGGTGTGAACCATGA GAAGTATG-3'

GADPH reverse: 5'-GGTGCAGGAGGCATTGCT-3'

### **Immunohistochemistry and immunofluorescence**

Paraffin-embedded tissue sections and frozen tissue sections were made by routine methods (<http://labs.fhcrc.org/fero/Protocols/processing.html>). For immunohistochemistry, Dako Envision two-step method of immunohistochemistry was used to stain CD31 (1:100 dilution) and  $\alpha$ -SMA (1:150 dilution) in xenograft tumor tissues as described previously (He et al. 2012a). Tissue sections were incubated with primary antibodies in a humid chamber overnight at 4°C. The microvessel density (MVD) reflected by CD31 positive staining was counted in three different fields per section. For immunofluorescence staining, frozen sections were incubated with primary antibodies overnight. Goat anti-rabbit or mouse IgG conjugated with FITC or TR (Santa Cruz Biotech, CA, USA) (1:200 dilution) were used as secondary antibodies and incubated for 2

h at room temperature. Slides were mounted with anti-fade DAPI reagent (Invitrogen, Grand Island, NY, USA).

### **ChIP-qPCR assay**

Chromatin immunoprecipitation assay (ChIP) was performed using EpiTect ChIP OneDay Kit (QIAGEN, Valencia, CA, USA) according to the manufacturer's instruction (<http://www.qiagen.com/products/catalog/assay-technologies/epigenetics/epitect-chip-oneday-kit>). HIF-1 $\alpha$  antibody (Abcam, Cambridge, MA, USA) was used to pull down the protein-chromatin complexes. Rabbit IgG was used as a negative control. The immunoprecipitated DNA was quantified using SYBR Green qPCR (Applied Biosystems). All results were normalized to 1% input value of the same sample. COX-2 primers flanking the hypoxia-response-elements (HRE) for SYBR Green qPCR:

Forward: 5'-TATACAGCCTATTAAGCGTCGTCA-3'

Reverse: 5'-CGTGTCTGGTCTGTACGTCTTTAG-3'

### **PGE<sub>2</sub> ELISA**

Cells were plated at  $0.1 \times 10^6$  cells/well of a 24-well plate, and allowed to recover overnight. The following day, the cells were replaced with fresh media and then cultured in normoxia or hypoxia (1% O<sub>2</sub>) for 24 h. The conditioned media were then collected and cleared of cellular debris by centrifugation at 2,000 rpm for 2 min. PGE<sub>2</sub> concentrations were determined using an ELISA kit as the manufacturer's instructions (<https://www.caymanchem.com/app/template/Product.vm/catalog/514010>) (Cayman, Ann Arbor, MI, USA).

### **miRNA luciferase reporter constructs and luciferase activity assay**

The 3'UTR-luciferase reporter constructs containing the 3'UTR regions of COX-2 with wild-type and mutant binding sites of miR-199a were amplified using PCR method (<http://www.promega.com/resources/protocols/product-information-sheets/g/gotaq-g2-flexi-dna-polymerase-protocol/>). The PCR products were cloned into the pMiR-luc luciferase reporter vector (Ambion, Grand Island, NY, USA). The mutant 3'UTR constructs were made by introducing 4 point mutations into the putative seed regions of COX-2. All the constructs containing 3'UTR inserts were sequenced and verified. The luciferase activity assay was performed as we previously described (He et al. 2013a).

### **Site-directed mutagenesis**

The human full-length COX-2 reporter used was a generous gift from Dr. Jian Li from Harvard University (Wu et al. 2006). To generate the HRE mutant COX-2 reporter, we performed site-directed mutagenesis on the wild type COX-2 reporter at the potential HIF-1 $\alpha$  binding sites with 3 bp substitutions as we previously described (Jiang et al. 1996). The mutant COX-2 reporter construct was validated by DNA sequencing.

### **Tube formation assay**

Human umbilical vein endothelial cells (HUVEC) were cultured in EBM-2 complete medium, and switched to EBM-2 basal medium containing 0.2% FBS for 24 h to perform tube formation assay. The conditioned media were prepared from different cells by replacing normal culture medium with serum-reduced medium (1% FBS). After culture for 24 h, the serum-reduced media were collected and stored at -20 C° for later use. The HUVEC cells were trypsinized, counted and resuspended in EBM-2 basic medium; then mixed with equal volume of the conditioned

medium and seeded on Matrigel-pretreated 96-well plate at  $2 \times 10^4$  cells/well. Tube formation was observed under light microscope after culture for 6-12 h, and photographed. The total lengths of the tubes for each well were measured using CellSens Standard software ([http://www.olympus-europa.com/microscopy/en/microscopy/components/component\\_details/component\\_detail\\_11457.jsp](http://www.olympus-europa.com/microscopy/en/microscopy/components/component_details/component_detail_11457.jsp)).

### **The CAM assay**

White Leghorn fertilized chicken eggs (Charles River, Malvern, PA, USA) were incubated at 37°C under constant humidity. Cells were transfected with miRNA precursors, or treated as specifically indicated in the figure legends. After transfection for 12 h, the cells were trypsinized, counted and resuspended in the serum-free medium. The cell suspensions were mixed with Matrigel at 1:1 ratio, and implanted onto the chorioallantoic membranes (CAM) of chicken eggs at Day 9. Tumor angiogenesis responses were analyzed 5 days after the implantation. The tumor/Matrigel plugs were trimmed off CAM, and photographed. The number of blood vessels as the index of angiogenesis was analyzed by counting the branches of blood vessels in three representative areas ( $1.5 \text{ mm}^2$ ) by two observers in a double blind manner.

### **miRNA transfection**

The negative control miRNA and miR-199a precursors were purchased from Applied Biosystems (Austin, TX, USA). Cells were cultured in 6-well plate to reach 60% confluency, and transfected using miR-199a or negative control precursor at 30 nM using Lipofectamine RNAiMAX reagent (Invitrogen, Grand Island, NY, USA) according to the manufacturer's instruction (<http://www.lifetechnologies.com/us/en/home/life-science/protein-expression-and-analysis/transfection-selection/lipofectamine-rnaimx.html>). Total proteins and RNAs were

prepared from the cells 60-70 h after the transfection, and followed by Western-blotting or RT-PCR analysis.

### **Hypoxia treatment**

Hypoxia incubator chamber (Stemcell, Vancouver, Canada) was used to generate hypoxia environment for cell culture. Cells were cultured in a hypoxia chamber (1% O<sub>2</sub>) for 24 h at 37°C.

### **Reactive oxygen species (ROS) study**

Cells were treated with ROS scavenger catalase (1500 U), or with H<sub>2</sub>O<sub>2</sub> (50 μM) for 12 h. Then cells were harvested, and total proteins were extracted for Western-blotting analysis.

### **Statistical analysis**

All the results were obtained from at least three independent experiments. Results were presented as mean ± SE and analyzed by Student's *t* test or One way ANOVA. All results were analyzed by SPSS for Windows, version 11.5. Differences were considered significant with  $P < 0.05$ .

## **Results**

### **miR-199a-5p is down-regulated in arsenic-transformed cells**

In order to investigate the mechanism of arsenic-induced carcinogenesis, we previous established an *in vitro* model by transforming immortalized human lung epithelial cell BEAS-2B via chronic exposure to 1 μM sodium arsenic for 26 weeks (Carpenter et al. 2011). The cell cultured in arsenic-free medium was served as passage-matched control. We performed miRNA microarray analysis to compare the miRNA profiles between parental cells (BEAS-2B) and arsenic-transformed cells (abbreviated as AsT). We found that miR-199a (referred to miR-199a-5p) was the most down-regulated among the list (data not shown). We further validated the result by

performing Taqman RT-qPCR analysis. As shown in Figure 1A, miR-199a was 100-fold lower in AsT cells, indicating a major change of miRNA abundance in cell malignant transformation. (He et al. 2013b). To investigate the relationship between arsenic treatment and miR-199a expression, we treated BEAS-2B cells with sodium arsenic at the dose of 0.5  $\mu\text{M}$ , 1  $\mu\text{M}$  and 2  $\mu\text{M}$  for 24 h. miR-199a expression levels were significantly decreased by arsenic treatment at the dose of 1  $\mu\text{M}$  and higher (Figure 1B). To determine whether cell transformation affects miR-199a expression, we used two different types of cell lines transformed by oncogenes. We tested PI3K-transformed chicken embryo fibroblast cells as was described (Chang et al. 1997; Jiang et al. 2000). miR-199a levels were decreased in transformed cells compared with its parental control cells, but the difference is not significant (see Supplemental Material, Figure S1). We also used newly transformed immortalized rat kidney cells RE3K by N-Ras (Kolligs et al. 1999) (see Supplemental Material, Figure S2A). We found that miR-199a expression levels in N-Ras-transformed cells were 1.9 fold lower compared to the control cells (see Supplemental Material, Figure S2B), indicating that transformation and/or oncogenes may decrease miR-199a expression. However, given that miR-199a expression levels were more than 100-fold lower in arsenic-transformed cells, we reason that arsenic plays a major role in the suppression of miR-199a expression.

### **miR-199a inhibits arsenic-induced angiogenesis *in vitro* and *in vivo***

Our earlier study showed that miR-199a processes an anti-angiogenic property in ovarian cancer cells (He et al. 2013a). We then investigated the functional effect of miR-199a in arsenic-induced angiogenesis by performing tube formation assay *in vitro*. As shown in Figure 2A, tube formation was strongly induced when cultured in conditioned medium prepared from AsT cells compared to its parental control B2B cells. Transient transfection of miR-199a in AsT cells

decreased tube formation by 40%. We next investigated the angiogenic effect of miR-199a in vivo. Firstly, we established AsT cells stably expressing miR-199a by transducing lentivirus carrying miR-199a-RFP. Then we generated xenograft tumors by the injection of stable cells AsT/miR-cont and AsT/miR-199a subcutaneously in nude mice and grew tumors for 6 weeks. Overexpression of miR-199a decreased the tumor weight by 50% compared with negative control cells (Figure 2B). The number of microvessels indicated by the endothelial marker CD31 staining in miR-199a-overexpressing tumors was significantly less than the control (Figure 2C). Like normal blood vessels, tumor vessels consist of endothelial cells, mural cells (pericytes and smooth muscle cells) and basement membrane (Baluk et al. 2003). The expression of  $\alpha$ -smooth muscle actin ( $\alpha$ -SMA) was restricted to vascular smooth muscle cells and co-localized with CD31 (Figure 2D). Interestingly, we noticed that blood vessels from AsT/miR-199a tumors had many more mural cells reflected by  $\alpha$ -SMA immunoreactivities than those from AsT/miR-cont tumors, suggesting that miR-199a decreases arsenic-induced tumor angiogenesis but promotes blood vessel maturation (Figure 2E).

### **miR-199a directly targets both HIF-1 $\alpha$ and COX-2**

Hypoxia-inducible factor 1 (HIF-1) is one of major pro-angiogenic factors through inducing transcriptional activation of vascular endothelial growth factor (VEGF) (Semenza 2000). Another potent angiogenic activator for tumor angiogenesis is cyclooxygenase 2 (COX-2), which is a rate-limiting enzyme in the conversion of arachadonic acid precursors in the cell membrane into prostaglandin E2 (PGE2) (Xue and Shah 2013). COX-2 and HIF-1 $\alpha$  expression are frequently regulated by the similar stimuli and control similar processes within the cells (Gately 2000; Liu et al. 1999). In the present study, we observed that basal levels of HIF-1 $\alpha$  and COX-2 under normoxia were markedly up-regulated in arsenic-transformed cells (Figure 3A). It was

reported that miR-199a directly targets HIF-1 $\alpha$  in cardiac myocytes (Rane et al. 2009). Indeed, overexpression of miR-199a in AsT suppressed HIF-1 $\alpha$  expression (Figure 3B). Interestingly, we noticed that miR-199a was also capable of downregulating COX-2 expression. To explore whether COX-2 can be directly targeted by miR-199a, we used “Target Search” to predict possible binding sites and free minimal energy of bindings and found that COX-2 is a putative target of miR-199a with two potential binding regions. COX-2 COX-2 3' UTR luciferase reporters containing two putative miR-199a binding sites were constructed to validate the direct binding between COX-2 mRNA 3'UTR and miR-199a. Co-transfection of miR-199a precursor with wild type reporter constructs containing binding sites (COX-2 3'UTR 311/320) greatly decreased the luciferase activities in B2B cells, while co-transfection with corresponding reporter containing point mutant at putative miR-199a binding sites did not affect the luciferase activities (Figure 3C). The luciferase activity in reporters containing putative binding sites in COX-2 3'UTR from 2021 to 2029 wasn't affected by miR-199a, which suggests that this computation-predicted site is not functionally targeted by miR-199a (Figure 3D). Consistently, the expression levels of COX-2 in xenograft tumors were generally lower in AsT/miR-199a groups than those in AsT/miR-cont groups (Figure 3E). These findings demonstrate that COX-2 is a novel direct target of miR-199a.

### **HIF-1 $\alpha$ directly regulates COX-2 at the transcriptional level**

We previously found that HIF-1 $\alpha$  can be strongly induced by acute arsenic treatment in prostate cancer cells under normoxia condition (Gao et al. 2004). In this study, we observed that both HIF-1 $\alpha$  and COX-2 expression levels were dramatically up-regulated in arsenic-transformed cells. We speculate whether there is an interaction between HIF-1 $\alpha$  and COX-2 in this context. It is known that the COX-2 promoter contains several HREs, one of which we predicted to be

functional (Jiang et al. 2009). In the present study, we first investigated whether HIF-1 $\alpha$  is required for arsenic-induced COX-2 expression. COX-2 mRNA and protein levels in B2B cells were upregulated under hypoxia condition, whereas knockdown of HIF-1 $\alpha$  by specific siRNA almost completely reversed the induction (Figs.4A-B). This indicates that hypoxia stimulates COX-2 expression via HIF-1 $\alpha$ . We further measured the concentration of COX-2 product, prostaglandin E<sub>2</sub> (PGE<sub>2</sub>) with the same treatments. Both B2B cells and AsT cells produced more PGE<sub>2</sub> under hypoxia. Conversely, knockdown of HIF-1 $\alpha$  decreased PGE<sub>2</sub> concentration with hypoxic treatment (Figure 4C). To determine if there is a direct interaction between HIF-1 $\alpha$  and COX-2 promoter, we performed chromatin immunoprecipitation (ChIP) assay. B2B cells were cultured in hypoxic chamber for 24h and were subjected to ChIP assay. As shown in Figure 4D, antibody against HIF-1 $\alpha$  was able to pull down COX-2 promoter suggesting the association between HIF-1 $\alpha$  and *COX-2* gene. The earlier findings in our group predicted that one of HRE (-576/-584) in the *COX-2* promoter would be functional (Jiang et al. 2009). We validated the binding sites by constructing COX-2 promoter luciferase reporters with wild type or mutant HRE. As shown in Figure 4E, hypoxia stimulated COX-2 transcriptional activity measured by luciferase activity in B2B cells transfected with wild type reporter. Conversely, B2B cells transfected with mutant reporter weren't affected by hypoxia. Furthermore, co-transfection of HIF-1 $\alpha$  with the wild type reporter similarly promoted COX-2 transcription while co-transfection with the mutant reporter did not affect the luciferase activities (Figure 4F). Collectively, these data support that HIF-1 $\alpha$  directly regulates COX-2 at the transcriptional level.

### **miR-199a inhibits arsenic-induced angiogenesis via COX-2 expression**

To determine the role of COX-2 in arsenic-induced angiogenesis, we knocked down COX-2 to evaluate the angiogenesis response by CAM assay (Figure 5A). We observed a dramatic

decrease of angiogenic potential in COX-2 knockdown cells (Figure 5B). To test whether the overexpression of COX-2 without miR-199a binding sites is able to reverse miR-199a-inhibited angiogenesis in AsT cells, we established stable AsT cells overexpressing COX2 by transducing lentivirus carrying COX-2 cDNA without 3'UTR region. We observed that forced expression of COX-2 completely reversed the inhibitory effect of miR-199a in angiogenesis (Figure 5C). Taken together, these results suggest that miR-199a inhibits arsenic-induced angiogenesis by directly targeting COX-2 expression.

### **Reactive oxygen species induce COX-2 pathway by suppressing miR-199a in arsenic-transformed cells**

Induction of reactive oxygen species (ROS) in cells is closely related with heavy metal exposure including arsenic, chromium and cadmium (Azad et al. 2010; Huang et al. 2004; Wang et al. 2012). We had observed that arsenic-transformed cells produced higher ROS (Carpenter et al. 2011). In addition, our earlier findings indicate that miR-199a is a ROS responsive miRNA in which ROS inhibit miR-199a expression through increasing the promoter methylation of miR-199a gene by DNA methyltransferase 1(He et al. 2012). In this study, we found that ROS treatment increased COX-2 expression, whereas ROS scavenger catalase decreased COX-2 expression (Figure 6A). To investigate whether ROS are upstream signals for inhibiting miR-199a expression, we treated AsT cells stably overexpressing miR-199a and AsT control cells with H<sub>2</sub>O<sub>2</sub>. We found that H<sub>2</sub>O<sub>2</sub> induced COX-2 expression in AsT/miR-cont cells, but no induction was observed in AsT/miR-199a cells (Figure 6B).

### **Discussion**

The strong links between the aberration of miRNAs profiles and carcinogenesis, cancer development, prognosis and chemo-resistance have been confirmed by a plethora of bench and

clinical studies (Iorio and Croce 2012). In this study, we identified that exposure to arsenic induced the suppression of miR-199a expression, which led to increased angiogenesis responses and tumor growth.

The process of angiogenesis normally occurs in the embryo, placenta and during menstrual cycle and wound-healing (Patella and Rainaldi 2012). However, under pathological situations such as cancer, the same angiogenic signaling pathways in tumors are induced in order to obtain the sufficient blood supply for tumor growth. A number of miRNAs have been reported to be involved in blood vessel development and angiogenesis by directly or indirectly regulating pro-angiogenic factors or anti-angiogenic factors (Hua et al. 2006; Poliseno et al. 2006; Urbich et al. 2008). Our previous study has showed that miR-199a inhibits tumor angiogenesis by targeting ERBB2 and ERBB3 thus suppressing their downstream VEGF in ovarian cancer cells. In the context of arsenic-induced transformation, miR-199a showed strong anti-angiogenic properties not only by directly targeting HIF-1 $\alpha$  but also another proangiogenic factor COX-2, which highlights the important role of miR-199a in angiogenesis. It is known that tumor vessels are leaky, immature, or morphologically abnormal due to the absent or incomplete basement membrane and mural cells (pericytes and smooth muscle cells). Failure of tumor vessels to recruit a normal coat of mural cells may contribute to the abnormality of vessels (Abramsson et al. 2002). Study showed that smooth muscle  $\alpha$ -actin ( $\alpha$ -SMA) expressing cells were present around capillaries, thus can act as pericyte marker (Berthod et al. 2012). Interestingly, we found that miR-199a can not only reduce the total number of microvessels in tumors but also promote vascular maturation indicated by the higher  $\alpha$ -SMA staining.

The HIF-1 $\alpha$  signaling plays a critical role in tumor metastasis, invasion, metabolism and especially angiogenesis (Covello and Simon 2004; Lum et al. 2007). We found that the base line of HIF-1 $\alpha$  expression level was dramatically up-regulated in arsenic-transformed cells, which is oxygen independent. The underlying mechanism might be activation of AKT, ERK, mTOR and p70S6K1 suggested by our earlier results (Carpenter et al. 2011). A recent study reported that overexpression of miR-199a inhibited the hypoxia-induced cell proliferation in non-small cell lung cancer by suppressing HIF-1 $\alpha$  (Ding et al. 2013). Oltipraz, a cancer chemopreventive agent, has anti-angiogenic property mediated by miR-199a induction and HIF-1 $\alpha$  inhibition (Kang et al. 2012). Consistent with the report, we showed that miR-199a suppression by arsenic exposure releases its direct target inhibition of HIF-1 $\alpha$ . More importantly, we also validated that COX-2 is a novel target of miR-199a and is functional in arsenic-transformed cells. The COX-2 expression was almost undetectable in parental BEAS-2B cells, but was pronouncedly expressed after chronic arsenic exposure. Our functional study revealed that COX-2 plays an important role in arsenic-induced angiogenesis which can be impaired by miR-199a overexpression. Furthermore, consistent with other studies (Csiki et al. 2006; Kaidi et al. 2006), both protein-DNA binding assay and luciferase reporter assay confirmed that HIF-1 $\alpha$  directly regulates COX-2 expression in parental BEAS-2B cells. This result along with data that PGE<sub>2</sub> can stimulate VEGF expression through the activation of HIF-1 $\alpha$  (Greenhough et al. 2009) suggests a positive-feedback between HIF-1 $\alpha$  and COX-2 in arsenic-induced angiogenesis. The findings also indicate that miR-199a may have high therapeutic efficiency as tumor suppressor by targeting both HIF-1 $\alpha$  and COX-2. In addition, it is worth noting that miR-199a-3p was also reported to target COX-2 in human chondrocytes (Akhtar and Haqqi 2012). Since miR-199a-3p and miR-199a-5p (miR-199a) are derived from the same gene, the expression levels of both miRNAs may

be somewhat regulated by the same mechanism(s). It is of interest to further investigate the upstream molecules which may indirectly modulate COX-2 expression via both miRNAs in the future.

Overproduction of reactive oxygen species (ROS) is closely related to heavy metal-mediated carcinogenesis (Lee et al. 2012). Oxidative stress was reported as a mediator of arsenic-induced cell transformation and carcinogenesis (Carpenter et al. 2011; Wang et al. 2012). In addition, ROS are able to activate HIF-1 $\alpha$  and COX-2 in various contexts (Bonello et al. 2007; Chen et al. 2012). However, the mechanism underlying ROS in regulating HIF-1 $\alpha$  and COX-2 still remains to be investigated. Here, we provide a link in which repression of miR-199a by arsenic-induced ROS activates HIF-1 $\alpha$  and COX-2 expression.

It is noted that we found that similar miR-199a suppression and HIF-1 $\alpha$ /COX-2 activation in Cr (VI)-transformed cells (see Supplemental Material, Figure S3). It is warranted for further investigation whether the same pathway is generally activated in other metal-induced cell transformation. Taken together, this study provides a new mechanism of arsenic-induced tumor angiogenesis and tumor growth. Arsenic-induced ROS inhibit miR-199a expression via DNMT1-mediated DNA methylation. The repression of miR-199a expression results in induction of HIF-1 $\alpha$  and COX-2. Additionally, the bi-directional regulations between HIF-1 $\alpha$  and COX-2 forming a positive feedback further promote tumor angiogenesis and tumor growth (Fig 6C). The findings may have clinical implication in targets therapy for arsenic-induced lung cancer in the future.

## References

- Abramsson A, Berlin O, Papayan H, Paulin D, Shani M, Betsholtz C. 2002. Analysis of mural cell recruitment to tumor vessels. *Circulation* 105:112-117.
- Akhtar N, Haqqi TM. 2012. MicroRNA-199a\* regulates the expression of cyclooxygenase-2 in human chondrocytes. *Ann Rheum Dis* 71:1073-1080.
- Azad N, Iyer A, Vallyathan V, Wang L, Castranova V, Stehlik C, et al. 2010. Role of oxidative/nitrosative stress-mediated Bcl-2 regulation in apoptosis and malignant transformation. *Ann N Y Acad Sci* 1203:1-6.
- Baluk P, Morikawa S, Haskell A, Mancuso M, McDonald DM. 2003. Abnormalities of basement membrane on blood vessels and endothelial sprouts in tumors. *Am J Pathol* 163:1801-1815.
- Beezhold K, Liu J, Kan H, Meighan T, Castranova V, Shi X, et al. 2011. miR-190-mediated downregulation of PHLPP contributes to arsenic-induced Akt activation and carcinogenesis. *Toxicol Sci* 123:411-420.
- Berthod F, Symes J, Tremblay N, Medin JA, Auger FA. 2012. Spontaneous fibroblast-derived pericyte recruitment in a human tissue-engineered angiogenesis model in vitro. *J Cell Physiol* 227:2130-2137.
- Boffetta P. 2004. Epidemiology of environmental and occupational cancer. *Oncogene* 23:6392-6403.
- Bonello S, Zahringer C, BelAiba RS, Djordjevic T, Hess J, Michiels C, et al. 2007. Reactive oxygen species activate the HIF-1alpha promoter via a functional NFkappaB site. *Arterioscler Thromb Vasc Biol* 27:755-761.
- Carpenter RL, Jiang Y, Jing Y, He J, Rojanasakul Y, Liu LZ, et al. 2011. Arsenite induces cell transformation by reactive oxygen species, AKT, ERK1/2, and p70S6K1. *Biochem Biophys Res Commun* 414:533-538.
- Chang HW, Aoki M, Fruman D, Auger KR, Bellacosa A, Tsichlis PN, et al. 1997. Transformation of chicken cells by the gene encoding the catalytic subunit of PI 3-kinase. *Science* 276:1848-1850.
- Chen CC, Cheng YY, Chen SC, Tuan YF, Chen YJ, Chen CY, et al. 2012. Cyclooxygenase-2 expression is up-regulated by 2-aminobiphenyl in a ROS and MAPK-dependent signaling pathway in a bladder cancer cell line. *Chem Res Toxicol* 25:695-705.

- Chen CL, Hsu LI, Chiou HY, Hsueh YM, Chen SY, Wu MM, et al. 2004. Ingested arsenic, cigarette smoking, and lung cancer risk: a follow-up study in arseniasis-endemic areas in Taiwan. *JAMA* 292:2984-2990.
- Covello KL, Simon MC. 2004. HIFs, hypoxia, and vascular development. *Curr Top Dev Biol* 62:37-54.
- Csiki I, Yanagisawa K, Haruki N, Nadaf S, Morrow JD, Johnson DH, et al. 2006. Thioredoxin-1 modulates transcription of cyclooxygenase-2 via hypoxia-inducible factor-1alpha in non-small cell lung cancer. *Cancer Res* 66:143-150.
- D'Amico TA. 2004. Angiogenesis in non-small cell lung cancer. *Semin Thorac Cardiovasc Surg* 16:13-18.
- Ding G, Huang G, Liu HD, Liang HX, Ni YF, Ding ZH, et al. 2013. MiR-199a suppresses the hypoxia-induced proliferation of non-small cell lung cancer cells through targeting HIF1alpha. *Mol Cell Biochem*. 2013 Sep 11. [Epub ahead of print]
- Gao N, Shen L, Zhang Z, Leonard SS, He H, Zhang XG, et al. 2004. Arsenite induces HIF-1alpha and VEGF through PI3K, Akt and reactive oxygen species in DU145 human prostate carcinoma cells. *Mol Cell Biochem* 255:33-45.
- Gately S. 2000. The contributions of cyclooxygenase-2 to tumor angiogenesis. *Cancer Metastasis Rev* 19:19-27.
- Greenhough A, Smartt HJ, Moore AE, Roberts HR, Williams AC, Paraskeva C, et al. 2009. The COX-2/PGE2 pathway: key roles in the hallmarks of cancer and adaptation to the tumour microenvironment. *Carcinogenesis* 30:377-386.
- He J, Xu Q, Wang M, Li C, Qian X, Shi Z, et al. 2012a. Oral administration of apigenin inhibits metastasis through AKT/P70S6K1/MMP-9 pathway in orthotopic ovarian tumor model. *Int. J. Mol. Sci* 13:7271-7282.
- He J, Jing Y, Li W, Qian X, Xu Q, Li FS, et al. 2013a. Roles and mechanism of miR-199a and miR-125b in tumor angiogenesis. *PLoS One* 8:e56647.
- He J, Qian X, Carpenter R, Xu Q, Wang L, Qi Y, et al. 2013b. Repression of miR-143 Mediates Cr (VI)-Induced Tumor Angiogenesis via IGF-IR/IRS1/ERK/IL-8 Pathway. *Toxicol Sci* 134:26-38.

- He J, Xu Q, Jing Y, Agani F, Qian X, Carpenter R, et al. 2012b. Reactive oxygen species regulate ERBB2 and ERBB3 expression via miR-199a/125b and DNA methylation. *EMBO Rep* 13:1116-1122.
- Hua Z, Lv Q, Ye W, Wong CK, Cai G, Gu D, et al. 2006. MiRNA-directed regulation of VEGF and other angiogenic factors under hypoxia. *PLoS One* 1:e116.
- Huang C, Ke Q, Costa M, Shi X. 2004. Molecular mechanisms of arsenic carcinogenesis. *Mol Cell Biochem* 255:57-66.
- Hubaux R, Becker-Santos DD, Enfield KS, Rowbotham D, Lam S, Lam WL, et al. 2013. Molecular features in arsenic-induced lung tumors. *Mol Cancer* 12:20.
- Iorio MV, Croce CM. 2012. MicroRNA dysregulation in cancer: diagnostics, monitoring and therapeutics. A comprehensive review. *EMBO Mol Med* 4:143-159.
- Jiang BH, Rue E, Wang GL, Roe R, Semenza GL. 1996. Dimerization, DNA binding, and transactivation properties of hypoxia-inducible factor 1. *J Biol Chem* 271:17771-17778.
- Jiang BH, Zheng JZ, Aoki M, Vogt PK. 2000. Phosphatidylinositol 3-kinase signaling mediates angiogenesis and expression of vascular endothelial growth factor in endothelial cells. *Proc Natl Acad Sci U S A* 97:1749-1753.
- Jiang Y, Cukic B, Adjeroh DA, Skinner HD, Lin J, Shen QJ, et al. 2009. An algorithm for identifying novel targets of transcription factor families: application to hypoxia-inducible factor 1 targets. *Cancer Inform* 7:75-89.
- Kaidi A, Qualtrough D, Williams AC, Paraskeva C. 2006. Direct transcriptional up-regulation of cyclooxygenase-2 by hypoxia-inducible factor (HIF)-1 promotes colorectal tumor cell survival and enhances HIF-1 transcriptional activity during hypoxia. *Cancer Res* 66:6683-6691.
- Kang SG, Lee WH, Lee YH, Lee YS, Kim SG. 2012. Hypoxia-inducible factor-1 $\alpha$  inhibition by a pyrrolopyrazine metabolite of oltipraz as a consequence of microRNAs 199a-5p and 20a induction. *Carcinogenesis* 33:661-669.
- Kolligs FT, Hu G, Dang CV, Fearon ER. 1999. Neoplastic transformation of RK3E by mutant beta-catenin requires deregulation of Tcf/Lef transcription but not activation of c-myc expression. *Mol Cell Biol* 19:5696-5706.
- Lee JC, Son YO, Pratheeshkumar P, Shi X. 2012. Oxidative stress and metal carcinogenesis. *Free Radic Biol Med* 53:742-757.

- Liu XH, Kirschenbaum A, Yao S, Stearns ME, Holland JF, Claffey K, et al. 1999. Upregulation of vascular endothelial growth factor by cobalt chloride-simulated hypoxia is mediated by persistent induction of cyclooxygenase-2 in a metastatic human prostate cancer cell line. *Clin Exp Metastasis* 17:687-694.
- Lum JJ, Bui T, Gruber M, Gordan JD, DeBerardinis RJ, Covelto KL, et al. 2007. The transcription factor HIF-1alpha plays a critical role in the growth factor-dependent regulation of both aerobic and anaerobic glycolysis. *Genes Dev* 21:1037-1049.
- Patella F, Rainaldi G. 2012. MicroRNAs mediate metabolic stresses and angiogenesis. *Cell Mol Life Sci* 69:1049-1065.
- Poliseno L, Tuccoli A, Mariani L, Evangelista M, Citti L, Woods K, et al. 2006. MicroRNAs modulate the angiogenic properties of HUVECs. *Blood* 108:3068-3071.
- Rahman MM, Chowdhury UK, Mukherjee SC, Mondal BK, Paul K, Lodh D, et al. 2001. Chronic arsenic toxicity in Bangladesh and West Bengal, India--a review and commentary. *J Toxicol Clin Toxicol* 39:683-700.
- Rane S, He M, Sayed D, Vashistha H, Malhotra A, Sadoshima J, et al. 2009. Downregulation of miR-199a derepresses hypoxia-inducible factor-1alpha and Sirtuin 1 and recapitulates hypoxia preconditioning in cardiac myocytes. *Circ Res* 104:879-886.
- Semenza GL. 2000. HIF-1: mediator of physiological and pathophysiological responses to hypoxia. *J Appl Physiol* 88:1474-1480.
- Urbich C, Kuehbach A, Dimmeler S. 2008. Role of microRNAs in vascular diseases, inflammation, and angiogenesis. *Cardiovasc Res* 79:581-588.
- Wang X, Mandal AK, Saito H, Pulliam JF, Lee EY, Ke ZJ, et al. 2012. Arsenic and chromium in drinking water promote tumorigenesis in a mouse colitis-associated colorectal cancer model and the potential mechanism is ROS-mediated Wnt/beta-catenin signaling pathway. *Toxicol Appl Pharmacol* 262:11-21.
- Wang Z, Zhao Y, Smith E, Goodall GJ, Drew PA, Brabletz T, et al. 2011. Reversal and prevention of arsenic-induced human bronchial epithelial cell malignant transformation by microRNA-200b. *Toxicol Sci* 121:110-122.
- Wu G, Luo J, Rana JS, Laham R, Sellke FW, Li J. 2006. Involvement of COX-2 in VEGF-induced angiogenesis via P38 and JNK pathways in vascular endothelial cells. *Cardiovasc Res* 69:512-519.

Xue X, Shah YM. 2013. Hypoxia-inducible factor-2alpha is essential in activating the COX2/mPGES-1/PGE2 signaling axis in colon cancer. *Carcinogenesis* 34:163-169.

## Figure legends

**Figure 1. miR-199a is down-regulated in arsenic- transformed cells.** (A) miR-199a expression levels were determined by Taqman RT-qPCR in AsT cells and B2B (refers to BEAS-2B) cells. (B) B2B cells were treated with sodium arsenic at different concentrations for 24 h. miR-199a expression levels were determined by RT-qPCR. Data are presented as mean  $\pm$  SE and analyzed by Student's *t* test. \* indicates significant decrease compared to that of control cells ( $P < 0.05$ ).

**Figure 2. miR-199a inhibits arsenic-induced angiogenesis.** (A) HUVEC cells were cultured in serum free medium overnight and re-suspended in basic EBM-2 medium. The conditioned media prepared from B2B, AsT or AsT transfected with miR-control or miR-199a precursor as indicated. Tube formation was determined and analyzed as described in Methods. Data represent means  $\pm$  SE from six replicates from each treatment, and are analyzed by One way ANOVA. \* indicate significant differences compared with B2B, whereas # indicate significant differences compared with AsT/miR-cont ( $P < 0.05$ ). Scale bar: 500  $\mu$ m. (B) Xenograft tumors from nude mice were established as described in Method section. Tumor weight was measured 6 weeks after cell injection. Data represent means  $\pm$  SE ( $n = 10$ /group). (C) Paraffin-embedded tumor tissue sections from both groups were used for immunohistochemical staining using antibodies against CD31. Top: representative sections. Magnification: 160 $\times$ . Scale bar: 50  $\mu$ m. Bottom: quantification of microvessel density (MVD) indicated by CD31 staining in tumor sections. Data represent means  $\pm$  SE from five different tumor sections from each group. (D) Frozen tissue sections were used for immunofluorescence staining. Magnification: 200 $\times$ . Scale bar: 50  $\mu$ m. (E) Paraffin-embedded tumor tissue sections were used for immunohistochemical staining using

antibodies against  $\alpha$ -SMA. Representative sections are shown. Arrow indicates mural cells. Magnification: 320 $\times$ . Scale bar: 50  $\mu$ m.

**Figure 3. miR-199a directly targets both HIF-1 $\alpha$  and COX-2.** (A) Total proteins prepared from AsT cells and B2B cells were used to determine protein levels of COX and HIF-1 $\alpha$  by Western-blotting. (B) AsT cells were transiently transfected with 25 nM miR-cont or miR-199a precursors for 72 h followed by Western-blotting assay. (C, D) Top: sequence alignment of human miR-199a sequence with 3' UTR region of COX-2. The luciferase reporter constructs were made as in Methods section, and relative luciferase activities were measured as indicated and normalized to those of the cells co-transfected with wild-type 3'UTR reporter and miRNA precursor control. Data are presented as mean  $\pm$  SE, and analyzed by Student's *t* test. \* indicates significant decrease compared to that of control cells ( $P < 0.05$ ). (E) COX-2 protein levels in tumor tissues ( $n = 10/\text{group}$ ) were determined by Western-blotting. Representative samples are shown.

**Figure 4. HIF-1 $\alpha$  directly regulates COX-2 expression at the transcriptional level.** (A, B) B2B cells were incubated under normoxic or hypoxic condition (1% O<sub>2</sub>) for 24 hours or transfected with 50 nM of a siRNA scramble control or a siRNA SMARTpool against HIF-1 $\alpha$  for 72h as indicated. The mRNA levels and protein levels of COX-2 were determined by SYBR-Green RT-qPCR or Western-blotting, respectively. (C) The concentrations of PGE<sub>2</sub> in B2B cells and AsT cells with indicated treatments were determined by ELISA method. (D) B2B cells were cultured under hypoxia for 24 hours and were subjected to ChIP assay using antibodies against IgG or HIF-1 $\alpha$ . The antibody-promoter binding signals were analyzed by SYBR-qPCR. (E) B2B cells were co-transfected with COX-2 luciferase reporters with wild type or mutant HIF-1 $\alpha$

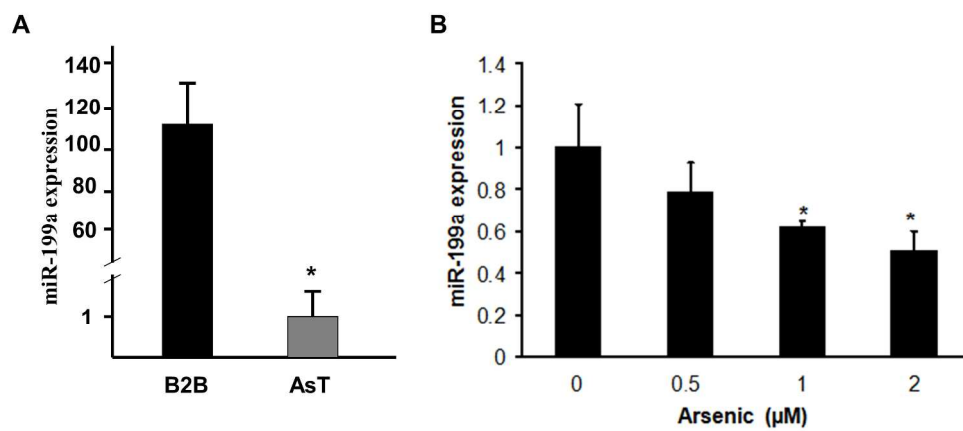
binding sites and  $\beta$ -gal plasmid. Cells were incubated under normoxia or hypoxia 24 hours before harvest. (F) B2B cells were co-transfected with COX-2 wide type or mutant reporters, HIF-1 $\alpha$  plasmid or vector and  $\beta$ -gal plasmid. Luciferase activity assay was performed 60 hours after transfection. Data are presented as mean  $\pm$  SE from three independent experiments and analyzed by One way ANOVA. \* indicates significant difference compared with the control ( $P < 0.05$ ).

**Figure 5. miR-199a inhibits As-induced angiogenesis via COX-2.** (A) AsT cells were transfected with 50 nM of a siRNA scramble control or a smartpool siRNAs against COX-2 for 60 h, followed by Western-blotting analysis. (B) AsT cells were transfected with a siRNA control or a siRNAs against COX-2 as above. The cells were implanted onto the CAMs 24 h after transfection to perform angiogenesis assay. Top: representative images from each group. Bottom: relative angiogenesis responses with mean  $\pm$  SE (n = 8/group). \*indicates significant difference compared with scrambled control ( $P < 0.01$ ). (C) AsT, AsT/vector or AsT/COX-2 cells were infected with miR-199a lentivirus for 24 hours. Then cells were used to perform angiogenesis assay. Top: representative images. Bottom: relative angiogenesis responses with mean  $\pm$  SE (n = 8). One way ANOVA was used to analyze the differences among various groups. \* indicates significant difference compared with miR-cont (AsT cells infected by lentivirus containing miR-cont).

**Figure 6. Excessive reactive oxygen species is an upstream of miR-199a/ COX-2 pathway in arsenic-transformed cells.** (A) AsT cells were treated with catalase (1500 U) or H<sub>2</sub>O<sub>2</sub> (50  $\mu$ M) for 12 hours followed by Western-blotting analysis. Bottom: quantification from three independent experiments using densitometry. (B) AsT cells stably expressing control or miR-

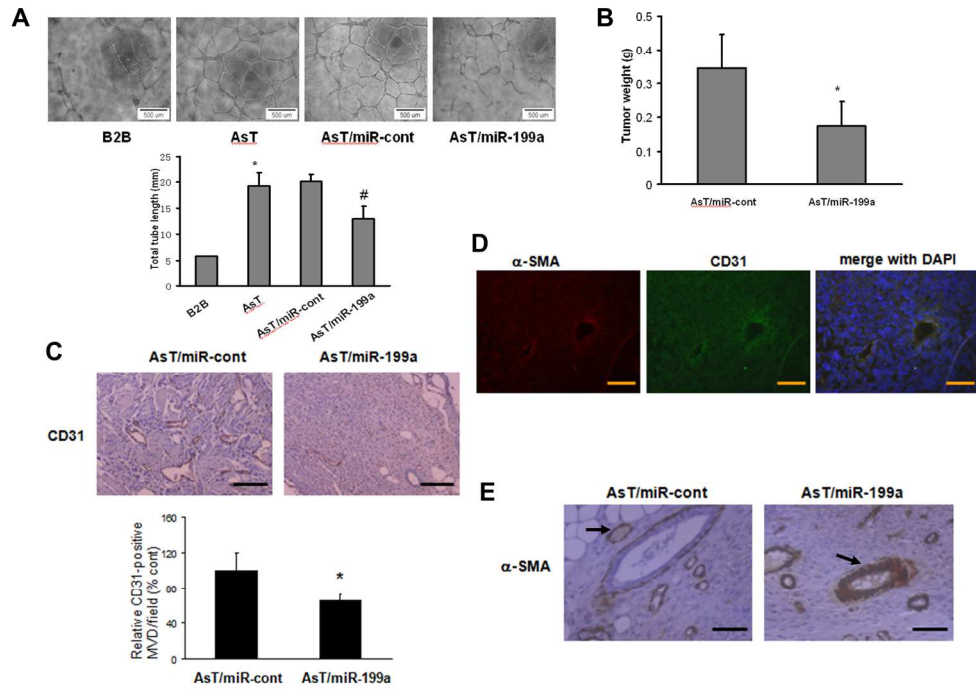
199a were treated with H<sub>2</sub>O<sub>2</sub> (50 μM) for 12 hours. COX-2 expression levels were determined by Western-blotting. Bottom: quantification from three independent experiments using densitometry. Student *t* test was used to determine the difference. \*indicates significant difference compared with control (P < 0.05). (C) Schematic diagram for proposed pathway.

He et al., Fig. 1



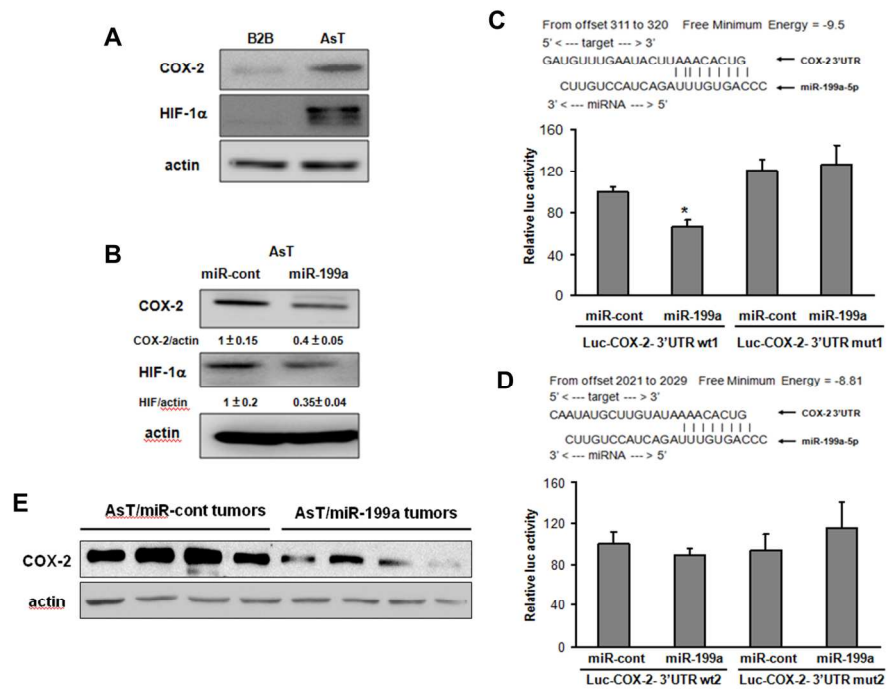
254x190mm (300 x 300 DPI)

He et al., Fig. 2



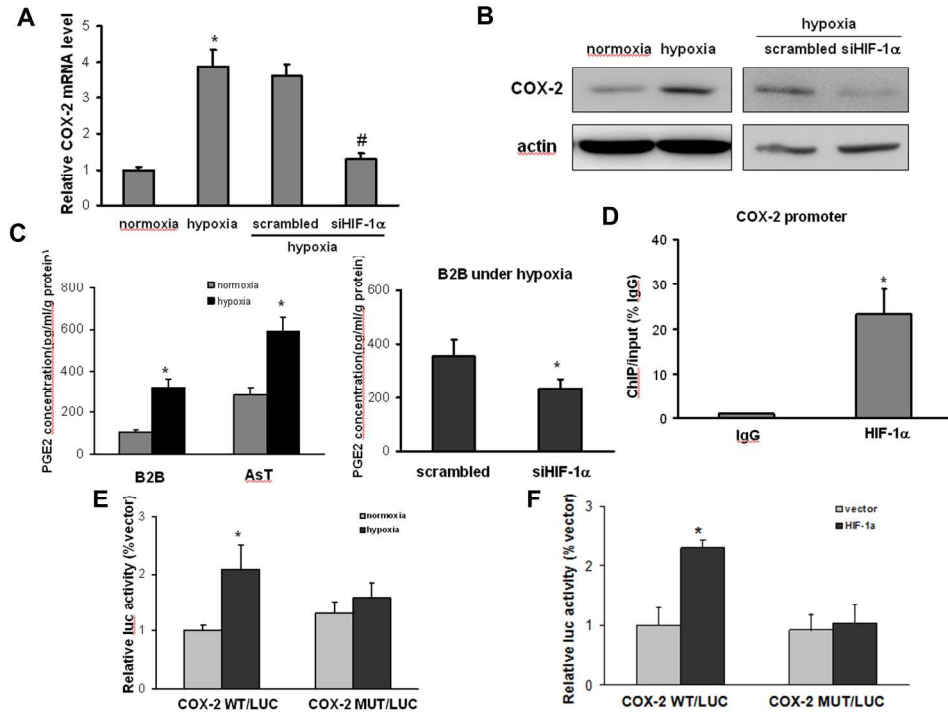
190x142mm (300 x 300 DPI)

He et al., Fig. 3



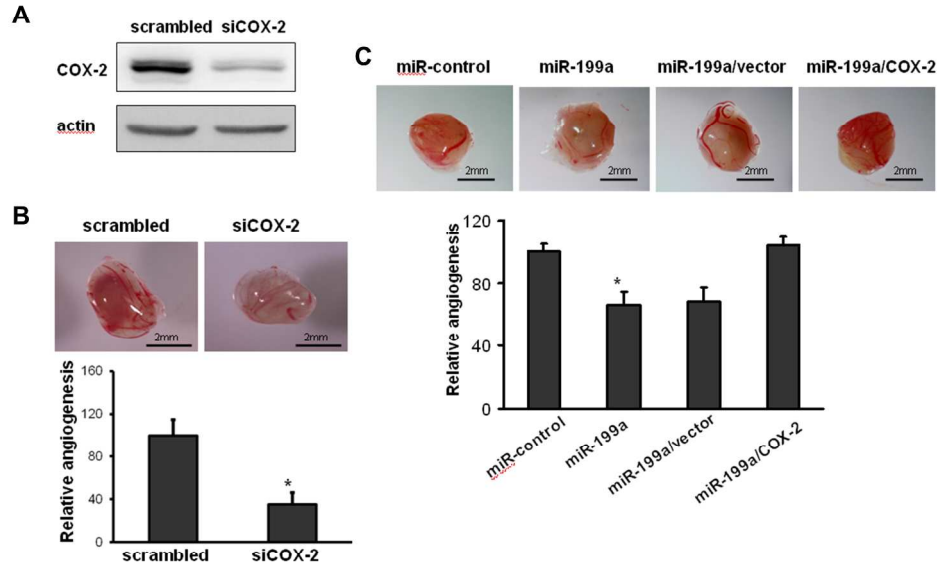
190x142mm (300 x 300 DPI)

He et al., Fig. 4



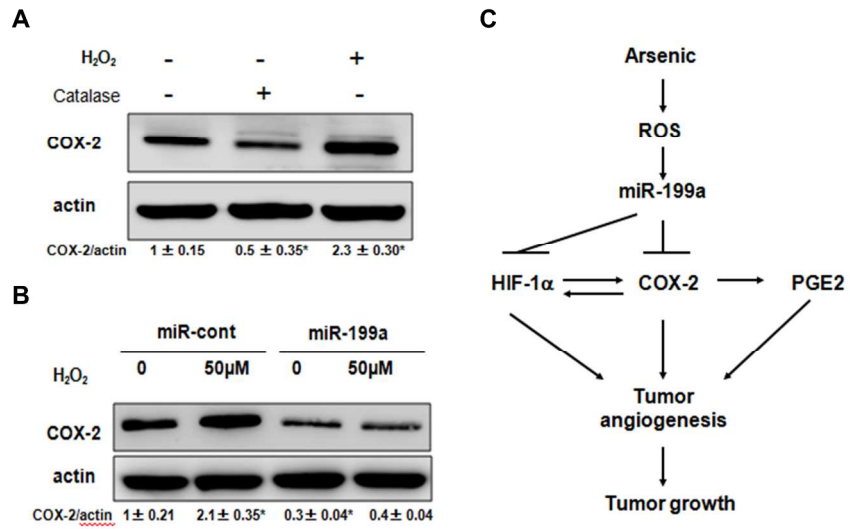
254x190mm (300 x 300 DPI)

He et al., Fig. 5



254x190mm (300 x 300 DPI)

He et al., Fig. 6



254x190mm (300 x 300 DPI)